Table IV. Rate Data for Neptunium(VI)–Sulfide Reaction at pH >10.5 and T = 25.0 °C

10^4[Np], M	10^3[Na_2S], M	k_1,[a] s^{-1}	pH	ionic strength, M
5.00	4.9	60.26 (±0.38)	11.53	0
5.00	4.9	60.92 (±0.45)	11.41	0.1
2.50	2.6	57.19 (±0.32)	11.18	0.1
2.50	2.4	58.28 (±1.42)	11.08	0.1
1.25	2.4	56.26 (±0.43)	11.23	0.1
1.25	1.2	53.74 (±0.64)	10.84	0.1

[a] Values in parentheses correspond to one standard deviation error limit.

10^{15} M^{-2} s^{-1}. The value for a is within 1.3 standard deviations of zero and so probably does not represent a real reaction pathway. As noted above, calculations indicate that the principal Np(VI)–hydroxide species in this pH regime is $NpO_2(OH)_3^-$. Since the $K_a[H^+]$ term in this pH range is much less than 1, [Na_2S] is equivalent to [HS^-] under these conditions. A rate law consistent with these observations can be derived from the mechanism

$$NpO_2(OH)_3^- + HS^- \overset{K_c'}{\rightleftharpoons} NpO_2(OH)_2SH^- + OH^- \quad (21)$$

$$NpO_2(OH)_2SH^- \xrightarrow{k_4} NpO_2(OH)_2^- + HS \quad (22)$$

The derived rate law is

$$-d[NpO_2(OH)_2SH^-]/dt = k_4K_c'/K_w[NpO_2(OH)_3^-][H^+][Na_2S] \quad (23)$$

where K_w is the ionization constant for water (1.66×10^{-14} M^{-2} at 0.1 M ionic strength). In this rate law, the empirical parameter b is equivalent to k_4K_c'/K_w, giving k_4K_c' = 49 (±8) s^{-1}. Because the dimensions of k_4K_c' are different from those of k_3K_c, the two parameters cannot be compared.

Conclusions

Both neptunium(VI) and plutonium(VI) are rapidly reduced by bisulfide ion in neutral to slightly alkaline solutions. The mechanism involves formation of a soluble sulfide complex followed by reduction of the hexavalent actinide ion in an intramolecular reaction. For plutonium, the rates of reaction are such that both the rate of the intramolecular reduction and the stability constant of the intermediate complex can be determined. The equivalent constants can be determined for neptunium at 25 °C but not at reduced temperatures. The rate of reduction of Np(VI) as a function of pH indicates two distinct reaction mechanisms at pH <10 and pH >10.5. The reaction rate is appreciably decreased but the reaction is not prevented by the presence of bicarbonate ions in the solution, implying that the postulated sulfide complex has considerable stability under these conditions. Further investigation of the nature of the sulfide complexes is planned.

Acknowledgment. This investigation was conducted under the auspices of the U.S. Geological Survey and the office of Basic Energy Sciences, Division of Chemical Sciences, U.S. Department of Energy, Contract No. W-31-109-ENG-38.

Registry No. Np, 7439-99-8; Pu, 7440-07-5; HS^-, 15035-72-0.

Supplementary Material Available: Tables containing the rate constants for all experiments for both plutonium and neptunium and the results of least-squares fits for several alternative mechanisms (22 pages). Ordering information is given on any current masthead page.

Contribution from the Department of Chemistry, York University, Downsview, Ontario M3J 1P3, Canada

Semiexhaustive Determination of Rate Parameters for Dissociative Axial Ligand Substitution in 24 Ferrous Dimethylglyoxime Complexes Involving 7 Different Axial Ligands

Xuening Chen and Dennis V. Stynes*

Received August 20, 1985

Syntheses, visible spectra, and kinetic data are presented for 24 of 28 possible complexes $Fe(DMGH)_2LT$ (L or T = methylimidazole (MeIm), pyridine (py), tributylphosphine (PBu_3), tributyl phosphite ($P(OBu)_3$), benzyl isocyanide (BzNC), tosylmethyl isocyanide (TMIC), and carbon monoxide). Axial ligand substitution reactions proceed via a dissociative mechanism in all cases. Dissociative rate constants spanning 8 orders of magnitude depend upon a leaving group order py > MeIm > $P(OBu)_3$ > PBu_3 ≥ CO > BzNC ≃ TMIC and a trans labilizing order py > MeIm > PBu_3 > $P(OBu)_3$ > BzNC ≥ TMIC > CO. The trans effect on MeIm and py dissociation correlates with the MLCT band in the visible spectrum, indicating that weakening of π bonding to the trans ligand constitutes a significant part of the barrier for dissociation. Relative rates of addition to the pentacoordinate intermediates cover about a factor of 10 and are independent of the trans ligand. The order of addition is similar to that found in hemes: MeIm ≃ BzNC ≃ TMIC > PBu_3 ≃ $P(OBu)_3$ > CO. Rates of dissociation of pyridines with substituents 4-CN, 3,4-Me_2, and 4-NMe_2 correlate with ligand basicity. Trans effects with increased donor strength of substituted pyridines are mildly accelerating for loss of σ donors and mildly decelerating for loss of CO. Relevance to other low-spin d^6 systems including hemes and Cr(0) complexes is discussed.

Introduction

Kinetic investigations of axial ligand substitution reactions of a variety of low-spin iron(II) complexes of the general form *trans*-FeN_4LT,[1] where N_4 is a planar tetradentate ligand such as bis(glyoxime),[2-4] porphyrin,[5,6] phthalocyanine,[7-9] or another macrocyclic ligand[10-14] and L and T monodentate ligands such

(1) Abbreviations: FeN_4, used in place of $Fe(DMGH)_2$ to designate bis(dimethylglyoximato)iron except when comparisons with other tetradentate ligands might lead to ambiguity; MeIm, 1-methylimidazole; Im, imidazole; BzNC, benzyl isocyanide; TMIC, tosylmethyl isocyanide; py, pyridine, 4-CNPy, 4-cyanopyridine; 3,4-Me_2Py, 3,4-dimethylpyridine; 4-Me_2NPy, 4-(dimethylamino)pyridine; MLCT, metal to ligand charge transfer. Rate constants are designated by k_{-L}^{T} for dissociation of the ligand L trans to T. The shortened forms N (MeIm), P (PBu_3), and PO ($P(OBu)_3$) are used as subscripts and superscripts.

(2) Pang, I. W.; Stynes, D. V. *Inorg. Chem.* **1977**, *16*, 59.
(3) Vaska, L.; Yamaji, T. *J. Am. Chem. Soc.* **1971**, *93*, 6673.
(4) Pomposo, F.; Stynes, D. V. *Inorg. Chem.* **1983**, *22*, 569.
(5) Weschler, C. J.; Anderson, D. L.; Basolo, F. *J. Am. Chem. Soc.* **1975**, *97*, 6707.
(6) White, D. K.; Cannon, J. B.; Traylor, T. G. *J. Am. Chem. Soc.* **1979**, *101*, 2443.
(7) Stynes, D. V.; James, B. R. *J. Am. Chem. Soc.* **1974**, *96*, 2733.
(8) Stynes, D. V. *Inorg. Chem.* **1977**, *16*, 1170.
(9) Martinsen, J.; Miller, M.; Trojan, D.; Sweigart, D. A. *Inorg. Chem.* **1980**, *19*, 2162.
(10) Stynes, D. V.; Hui, Y. S.; Chew, V. *Inorg. Chem.* **1982**, *21*, 1222.

0020-1669/86/1325-1173$01.50/0

as imidazoles, pyridine, CO, RNC, PR_3, etc. have shown that a classic dissociative mechanism is operative in these systems. Large differences in rates as a function of the *cis*-N_4 ligand, trans ligand T, or leaving group L are found.

Pentacoordinate intermediates have been probed directly for hemes by using flash photolysis methods,[5,15-20] and rates of addition of ligands are fast ($k_{+E} \simeq 10^7$ to 10^8 M^{-1} s^{-1} at 25 °C). In other systems relative rates of addition of ligands determined by using competitive methods have indicated that the pentacoordinate intermediate shows little discrimination among different entering ligands.[6-8]

The $Fe(DMGH)_2$ system is especially attractive as a vehicle to explore axial ligation to low-spin iron(II) in detail since characteristic MLCT bands are observed and these are especially sensitive to changes in axial ligands as well as changes in the oxime (benzoquinone[4] and naphthoquinone[21] dioxime complexes for example). Like hemes, these complexes are neutral and soluble in nonpolar solvents. They also undergo photochemical substitution reactions,[22] which will be described in detail elsewhere.

Herein we present an exhaustive study of 24 of the 28 possible complexes $Fe(DMGH)_2LT$ for L or T = methylimidazole (MeIm), pyridine (py), tributylphosphine (PBu_3), tributyl phosphite ($P(OBu)_3$), benzyl isocyanide (BzNC), tosylmethyl isocyanide (TMIC), or carbon monoxide, kinetic data for 35 of the 49 possible dissociation rates, and a survey of relative rates of ligand additions to three of the seven possible pentacoordinate intermediates.

This data provides a definitive characterization of the trans effects and leaving group order, which to a large extent are transferable to other FeN_4 systems. For the remainder of this paper the abbreviation FeN_4 will be used for the $Fe(DMGH)_2$ system.

Experimental Section

Materials. $FeN_4(py)_2$, $FeN_4(MeIm)_2$, $FeN_4(MeIm)(CO)$, and $FeN_4(BzNC)_2$ were available from previous work.[2] FeN_4L_2, L = 4-CNPy, 3,4-Me_2Py, and 4-Me_2NPy, were prepared by literature methods.[23] All ligands and solvents were from standard sources and used as received.

Physical Measurements. Visible spectra were recorded on an Aminco DW-2a UV/vis spectrophotometer. NMR spectra were obtained on a Bruker AM300 instrument with an Aspec 3000 computer using deuteriochloroform as solvent with 0.1% Me_4Si as an internal standard. Elemental analyses were performed by Canadian Microanalytical Service Ltd., Vancouver, BC.

Syntheses. All syntheses were carried out under a nitrogen atmosphere.

$FeN_4(PBu_3)(MeIm)$. To a solution of 40 mL of chloroform, 0.4 mL of tributylphosphine, and 5 mL of methanol was added 1.0 g of $FeN_4(MeIm)_2$ to give a pink solution. The mixture was stirred for 15 min and filtered. The filtrate was evaporated to about 10 mL. The product was crystallized from an ice-cold solution of 10 mL of acetone and 5 mL of water and dried in vacuo. Anal. Calcd for $C_{24}H_{47}N_6PO_4Fe$: C, 50.53; H, 8.30; N, 14.73. Found: C, 49.97; H, 8.04; N, 15.14. NMR: δ 0.87 (PBu_3, CH_3), 1.2 (m, PBu_3, $CH_2CH_2CH_2$), 2.31 (DMGH, CH_3), 3.53 (MeIm, CH_3), 6.57, 6.84, 7.28 (MeIm, C–H).

$FeN_4(P(OBu)_3)(MeIm)$. To a solution of 0.16 mL of tributyl phosphite, 30 mL of chloroform, and 5 mL of methanol was added 1.0 g of $FeN_4(MeIm)_2$. The mixture was stirred for 15 min and then filtered. The filtrate was evaporated to 4 mL. Crystals were obtained from petroleum ether (30–60 °C). The product was dried in vacuo. Anal. Calcd for $C_{24}H_{47}N_6O_7Fe$: C, 46.61; H, 7.66; N, 13.59. Found: C, 45.55; H, 7.39; N, 15.02. NMR: δ 0.89 ($P(OBu)_3$, CH_3), 1.32–1.47 ($P(OBu)_3$, CH_2–CH_2), 2.18 (DMGH, CH_3), 3.55 (MeIm, CH_3), 3.77 ($P(OBu)_3$, O–CH_2), 6.61, 6.96, 7.4 (MeIm, CH).

$FeN_4(P(OBu)_3)_2$. A solution of 1.2 mL of $P(OBu)_3$, 30 mL of chloroform, and 1.0 g of $FeN_4(py)_2$ was refluxed for 1/2 h. The solution was filtered and evaporated to almost dryness in a hot water bath (90–100 °C). The residue was dissolved in 5 mL of hexane and left in the freezer overnight, giving red-orange crystals, which were washed with 15 mL of ice-cold hexane and dried in vacuo. Anal. Calcd for $C_{32}H_{54}N_4P_2O_{10}Fe$: C, 48.86; H, 8.71; N, 7.12. Found: C, 48.13; H, 8.44; N, 8.62. NMR: δ 0.88 ($P(OBu)_3$, CH_3), 1.30 ($P(OBu)_3$, CH_2), 1.45 ($P(OBu)_3$, CH_2), 2.15 (DMGH, CH_3), 3.78 ($P(OBu)_3$, O–CH_2).

$FeN_4(PBu_3)_2$ was also prepared from $FeN_4(py)_2$ and crystallized from acetone–water. The product gave satisfactory elemental analysis and NMR data.

In Situ Generation of Species. Species generated in situ were in all cases products of a clean reaction with known rates monitored by visible spectroscopy. λ_{max} is given in Table I.

$FeN_4L(CO)$ (L = PBu_3, $P(OBu)_3$). Toluene solutions of FeN_4L_2 were saturated with CO and allowed to stand at 60 °C. Spectra with time gave clean isosbestic points and a rate process consistent with k_{-L}^{L}, resulting in characteristic spectra of the carbonyl derivative.

$FeN_4(PBu_3)(P(OBu)_3)$. A toluene solution of 10^{-4} M $FeN_4(PBu_3)_2$ containing $\sim 10^{-3}$ M $P(OBu)_3$ was monitored with time at 60 °C. Spectra showed clean isosbestic points and pseudo-first-order rate constant k_{-P}^{P}. The second step to give FeN_4 ($P(OBu)_3)_2$ is slow.

$FeN_4(PR_3)(R'NC)$ (R = Bu or OBu, R' = Benzyl or Tosylmethyl). Toluene solutions of $FeN_4(PR_3)_2$ were reacted with R'NC. Spectra monitored with time at 60 °C showed clean isosbestic points and a pseudo-first-order rate constant k_{-P}^{P} or k_{-PO}^{PO}. The second step to give $FeN_4(RNC)_2$ is slow.

$FeN_4(BzNC)(CO)$. A CO-saturated toluene solution of $FeN_4(BzNC)_2$ in a 1-cm optical glass cell was irradiated for 5 min with white light from a 200-W quartz–halogen lamp. Clean spectral changes with an isosbestic point at 369 nm indicated formation of the carbonyl complex. Subsequent reaction with BzNC afforded a return to the spectrum of the original $FeN_4(BzNC)_2$ solution (k_{-CO}^{BzNC}). Reaction with MeIm gave $FeN_4(MeIm)(BzNC)$ and $FeN_4(MeIm)_2$ as expected.

$FeN_4(MeIm)(TMIC)$. Solid $FeN_4(MeIm)_2$ was added to a toluene solution of TMIC and left standing at room temperature for 30 min. The resulting mixture was filtered to remove undissolved $FeN_4(MeIm)_2$.

$FeN_4(L)(PR_3)$ (L = 4-CNPy, py, or 4-NMe_2Py; R = Bu or OBu). Solid $FeN_4(L)_2$ was added to a toluene solution of the phosphorus ligand and left to stand until the characteristic visible spectrum of the product (Table III) was obtained.

Kinetics. Reactions in which CO was the entering ligand were carried out under 1 atm of CO. Otherwise all reactions were routinely run in serum-capped nitrogen-purged cuvettes and monitored by visible spectroscopy. Temperatures were maintained by means of water circulation through a thermostatable cell holder. Temperatures were read directly from a RTD device attached to the cell holder.

Reaction solutions were prepared either by injecting 10–100 μL of the ligand (either neat or as a toluene solution) into a thermostated solution of the complex in a cuvette or by injecting 10–100 μL of a more concentrated solution of the complex into a thermostated toluene solution of the ligand. Concentrations of the complexes were typically 10^{-4} M.

Rate constants for reactions involving a single pseudo-first-order rate were obtained from a least-squares fit of log $[(A - A_\infty)/(A_0 - A_\infty)]$ vs. time using a microcomputer. Data covering 3 half-lives were analyzed for 20 values of A_∞. The best fit value of A_∞ typically corresponded to

Table I. Visible Spectral Data for FeN_4XY Complexes in Toluene Solution

	λ_{max}, nm					
	py	MeIm	PBu_3	$P(OBu)_3$	BzNC	TMIC
py	508, 422					
MeIm	519, 419	531				
PBu_3	492, 374	499	468			
$P(OBu)_3$	459, 368	460	436	414		
BzNC	444, 345	447	425	399	392	
TMIC	430, 338	428	414	392		
CO	389, 350	385	376	360	350	

(11) Kildahl, N. K.; Lewis, T. J., Antonopoulos, C. *Inorg. Chem.* **1981**, *20*, 3952.
(12) Kildahl, N. K.; Balkus, K.J., Jr.; Flynn, M. J. *Inorg. Chem.* **1983**, *22*, 589.
(13) Butler, A.; Linck, R. G. *Inorg. Chem.* **1984**, *23*, 2227.
(14) Butler, A.; Linck, R. G. *Inorg. Chem.* **1984**, *23*, 4545.
(15) Lavalette, D.; Tetreau, C.; Momenteau, M. *J. Am. Chem. Soc.* **1979**, *101*, 5395.
(16) Traylor, T. G.; Tsuchiya, S.; Campbell, D.; Mitchell, M.; Stynes, D. V.; Koga, N. *J. Am. Chem. Soc.* **1985**, *107*, 604.
(17) Stanford, M. A.; Swartz, J. C.; Phillips, T. E.; Hoffman, B. M. *J. Am. Chem. Soc.* **1980**, *102*, 4492.
(18) Collman, J. P.; Brauman, J. I.; Iverson, B. L.; Sessler, J. L.; Morris, R. M.; Gibson, Q. H. *J. Am. Chem. Soc.* **1983**, *105*, 3052.
(19) Ward, B.; Wang, C.; Chang, C. K. *J. Am. Chem. Soc.* **1981**, *103*, 3052.
(20) Olson, J. S.; McKinnie, R. E.; Mims, M. P.; White, D. K. *J. Am. Chem. Soc.* **1983**, *105*, 1522.
(21) Siddiqui, N.; Stynes, D. V., to be submitted for publication.
(22) (a) Irwin, C.; Stynes, D. V. *Inorg. Chem.* **1978**, *17*, 2882. (b) Chen, X.; Stynes, D. V., to be submitted for publication.
(23) Yamano, Y.; Masuda, I.; Shinra, K. *Bull. Chem. Soc. Jpn.* **1971**, *44*, 1581.

Table II. Rate Constants for Dissociation of L Trans to T for FeN_4TL[a]

		10^4k, s^{-1}					
L	*T*, °C	T = py	T = MeIm	T = PBu_3	T = $P(OBu)_3$	T = BzNC	T = TMIC
py	10	87	48				
	45			250	12	0.23[b]	0.064[b]
MeIm	10	2.5	5.2				
	25		62	0.77			
	45		890	19	0.65		
	60			158	5.7	0.1[b]	<0.1
	70				25		
PBu_3	60	13	13	7.5	0.2		
	80					0.23	<0.1
$P(OBu)_3$	60	92	68	40	15		
	80					5 (1)	
BzNC	65	4.6[c]	3.1[c]				
	80			34	2.1	0.6 (1)	
TMIC	80	80	15	12	1.4		
CO	60	20[b]	5.2	230	160	15	

[a] Error in last digit in parentheses, otherwise ±5%. [b] Calculated from ΔH^* and ΔS^* in Table IV. [c] Reference 2.

Table III. Spectroscopic and Kinetic Data for Substituted Pyridine Derivatives in Toluene

		L			
	T, °C	4-NMe_2Py	3,4-Me_2Py	py	4-CNPy
pK_a[a]		9.7	6.8	5.2	1.8
		Spectra:[b] λ_{max}, nm			
FeN_4L_2		542, 370	517, 407	508, 422	498, 530
$FeN_4L(py)$		522, ~380, ~430	514, ~412	508, 422	498, ~535, 390
$FeN_4L(CO)$		~390, <340		389, 350	372, <340
$FeN_4L(P(OBu)_3)$		466, <330	462, ~350	459, 368	456
$FeN_4L(PBu_3)$		506, <350	497, 368	492, 374	470, ~480
		Rates: 10^4k, s^{-1}			
k_{-py}^{L}	10	110	80	44[c]	24
k_{-PO}^{L}	60	110		92	*d*
k_{-CO}^{L}	60	12		20	75
k_{-L}^{L}	10	8.0	44	87	93
k_{-L}^{PO}	45	0.7	7.9	12	46
k_{-L}^{P}	45	16	110	250	1000

[a] Reference 44. [b] λ_{max} listed in order of assignment: charge transfer to oximes, to substituted pyridine, and to pyridine. [c] Value of k_{-py}^{py} in Table II corrected by factor of 2 for statistical effect. [d] Reaction with excess 4-CNPy does not go to completion; other entering ligands give initial replacement of L.

that measured experimentally after 7 half-lives. In cases where a second reaction or other complications prevented a direct determination of A_∞, the value obtained from the least-squares fit was used.

For reactions involving two consecutive first-order rates of comparable magnitude, absorbance data vs. time at several wavelengths were analyzed by computer comparison of observed and calculated absorbances. A_{calcd} was obtained from the equation $A_{calcd} = A_0(\alpha_1) + A_2(\alpha_2) + A_\infty(\alpha_3)$ where α_1, α_2, and α_3 are the fractions of three species involved vs. time[24] and A_0, A_2, and A_∞ are the absorbances of a solution of 100% of species **1**, **2**, and **3**, respectively, at the wavelength and the concentration of total iron complex used. A_0 and A_∞ were obtained directly from the initial and final spectra. Absorbances vs. time were calculated for various values of the two rate constants, k_1 and k_2, and the absorbance of the middle species (A_2). Typically a 10 × 10 × 10 array of deviations was inspected for the minimum and to spot correlation problems. Values of k_1, k_2, and A_2 with deviations within a factor of 2 of the global minimum were considered acceptable solutions. In some cases an independent determination of A_2 was used to place additional constraints on the solution.

Results

The new complexes $FeN_4(PBu_3)_2$, $FeN_4(MeIm)(PBu_3)$, $FeN_4(P(OBu)_3)(MeIm)$, and $FeN_4(P(OBu)_3)_2$ were obtained as crystalline solids and characterized by NMR, visible spectroscopy, and elemental analysis. Other derivatives were generated in situ and are characterized by their visible spectra and clean reactions involving axial ligand substitution.

Visible spectral data for the FeN_4XY complexes for X or Y being any one of seven possible ligands are given in Table I. The single absorption maximum in the visible region is assigned to a MLCT involving a π^* level of the oxime ligand.[2,23,25] The λ_{max} value correlates with the π-acceptor character of the axial ligands consistent with (XZ, YZ) → π^* excitation. The expected greater π-acceptor character of ligands with electron-withdrawing substituents is demonstrated for $P(OBu)_3$, PBu_3 and TMIC, BzNC. The order of π-acceptor strength deduced here is consistent with that generally assumed on the basis of other data in organometallic complexes of these ligands.[26]

Kinetics. For a ligand substitution reaction

$$FeN_4TL + E \rightarrow FeN_4TE + L \quad (1)$$

involving entering group E, leaving group L, and trans ligand T and proceeding via a dissociative mechanism (D)

$$FeN_4TL \underset{k_{+L}^{T}}{\overset{k_{-L}^{T}}{\rightleftharpoons}} FeN_4T \underset{k_{-E}^{T}}{\overset{k_{+E}^{T}}{\rightleftharpoons}} FeN_4TE \quad (2)$$

the pseudo-first-order rate constant for approach to equilibrium is given by

$$k_{obsd} = \frac{k_{-L}k_{+E}[E] + k_{-E}k_{+L}[L]}{k_{+L}[L] + k_{+E}[E]} \quad (3)$$

For [L] negligible and [E] large, the expression reduces to $k_{obsd} = k_{-L}$ and the reaction gives 100% FeN_4TE with a rate independent of the concentration or nature of the entering group E. These conditions are used to obtain "off rates".

(24) Frost, A. A.; Pearson, R. G. "Kinetics and Mechanism", 2nd ed.; Wiley: New York, 1962; pp 166–167.
(25) Jillot, B. A.; Williams, R. J. P. *J. Chem. Soc.* **1958**, 462.
(26) Atwood, J. D. "Inorganic and Organometallic Reaction Mechanism"; Brooks Cole: Monterey, CA 1985; p 104.

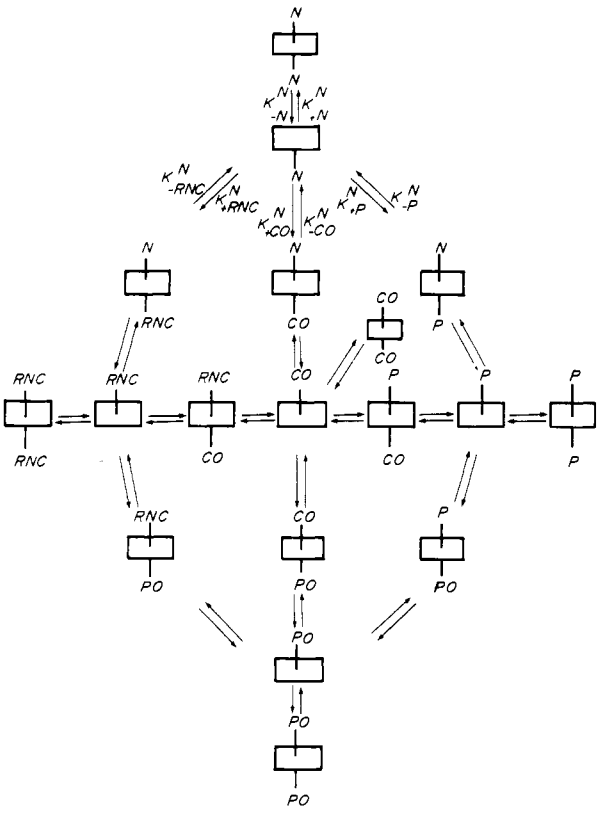

Figure 1. Reaction scheme showing the reactions of the 13 complexes FeN_4XY and five pentacoordinate intermediates for five different ligands MeIm, PBu_3, $P(OBu)_3$, RNC, and CO. The symbolism used for on and off rates is indicated for the trans ligand N.

If the reaction is studied in the presence of a pseudo-first-order excess of both L and E, relative rates of addition of L vs. E to the pentacoordinate intermediate FeN_4T may be obtained from the dependence of k_{obsd} on the ratio [E]/[L]:

$$k_{obsd} = \frac{\dfrac{k_{-L}}{k_{+L}[L]} + k_{-E}}{1 + \dfrac{k_{+E}[E]}{k_{+L}[L]}} \qquad (4)$$

Two cases arise. If k_{-E} is negligible, the reaction goes to completion and a plot of $1/k_{obsd}$ vs. [L]/[E] is a straight line. If k_{-E} cannot be neglected, one obtains a first-order approach to equilibrium and plots $1/(k_{obsd} - k_{-E})$ vs. [L]/[E]. In either case values of k_{-L} and k_{+L}/k_{+E} are obtained from a linear least-squares fit of the data. The rate constants k_{+L} and k_{+E} will be referred to as "on rates".

The overall equilibrium constant, K, for reaction 1 is related to the "on" and "off" rate constants:

$$K = \frac{k_{-L}{}^{T} k_{+E}{}^{T}}{k_{-E}{}^{T} k_{+L}{}^{T}} \qquad (5)$$

The equilibrium constant can be independently obtained from spectroscopic data by standard methods providing a check of the rate data and the presumed D mechanism.

The existence of a classic D mechanism greatly simplifies the description of the reaction rates. For example, since the rate is independent of the nature of the entering group E, the number of rate constants required to specify *all* substitution reactions for seven different ligands T, E, and L is reduced from 343 to only 98 (49 off rates and 49 on rates). We have obtained 35 of the off rates (the off rates trans to CO could not be obtained since in all cases CO is replaced in preference to the ligand trans to CO) For reactions carried out under limiting conditions where $k_{obsd} = k_{-L}$, only the 49 off rates are required to describe the 343 possible reaction rates.

Off Rates. Figure 1 illustrates the relationship between some of the complexes and intermediates investigated. The kinetic data for reactions of FeN_4XY derivatives are most easily summarized by referring to the array of rate constants given in Table II. The seven ligands considered in this work are arranged in order of generally decreasing trans effect from left to right and generally decreasing leaving group order from top to bottom (note that PBu_3 is an exception). Reaction of a complex FeN_4L_2 with entering ligand E will proceed in two distinct steps if E lies lower in the trans effect series than L. For example reaction of $FeN_4(CH_3Im)_2$ with $P(OBu)_3$ results in a clean reaction to give $FeN_4(CH_3Im)(P(OBu_3)$. Subsequent reaction to give $FeN_4(P(OBu)_3)_2$ is much slower. If E lies to the left of L in the trans effect series, the middle species is typically not detected and a single rate process to give $FeN_4(E)_2$ with clean isosbestic points is observed. For example reaction of $FeN_4[P(OBu)_3]_2$ with PBu_3 goes directly to the $FeN_4(PBu_3)_2$ complexes with no significant buildup of the $FeN_4(PBu_3)(P(OBu)_3)$ intermediate. When the two rates are comparable, no isosbestic points are observed and the spectra were analyzed at several wavelengths by using a least-squares approach in which absorbances were calculated for various values of k_1, k_2, and ϵ_2 (the two rate constants and the extinction coefficient of the intermediate species). The least-squares fit typically gave a well-defined minimum at one or more wavelengths, and the derived values of k_1 or k_2 and ϵ_2 were typically in good agreement with values obtained from simple single-step reactions using a different entering ligand or starting from the middle species.

Thus rates of reactions 6–8 afford the rate constants shown in clean single-step reactions. Reactions 9 and 10 show little to no

$$FeN_4(MeIm)(PR_3) + MeIm \xrightarrow{k_{-P}{}^{N}} FeN_4(MeIm)_2 + PR_3 \quad (6)$$
R = Bu or OBu

$$FeN_4(MeIm)(PR_3) + PR_3 \xrightarrow{k_{-N}{}^{P}} FeN_4(PR_3)_2 + MeIm \quad (7)$$
R = Bu or OBu

$$FeN_4(PBu_3)_2 + P(OBu)_3 \xrightarrow{k_{-P}{}^{P}} FeN_4(PBu_3)(P(OBu)_3) + PBu_3 \quad (8)$$

$$FeN_4(P(OBu)_3)_2 + 2PBu_3 \xrightarrow{k_{-PO}{}^{PO}} FeN_4(PBu_3)_2 + 2P(OBu)_3 \quad (9)$$

$$FeN_4(BzNC)_2 + 2PBu_3 \xrightarrow{k_{-BzNC}{}^{BzNC}} FeN_4(PBu_3)_2 + 2BzNC \quad (10)$$

buildup of the middle species and give the single rate constant shown. Reactions 11–13 proceed via two consecutive first-order

$$FeN_4(PBu_3)_2 + MeIm \xrightarrow{k_{-P}{}^{P}} FeN_4(MeIm)(PBu)_3 \xrightarrow{k_{-P}{}^{N}} Fe(MeIm)_2 \quad (11)$$

$$FeN_4(MeIm)_2 + py \xrightarrow{k_{-N}{}^{N}} FeN_4(MeIm)(py) \xrightarrow{k_{-N}{}^{py}} FeN_4(py)_2 \quad (12)$$

$$FeN_4(py)_2 + MeIm \xrightarrow{k_{-py}{}^{py}} FeN_4(MeIm)(py) \xrightarrow{k_{-py}{}^{N}} FeN_4(MeIm)_2 \quad (13)$$

rates of comparable magnitude without isosbestic points. Reactions 12 and 13 were subjected to a detailed analysis. Let k_1 and k_2 denote rate constants for the first and second steps of reaction 12 and 13. The two-rate analysis of the spectral data gave acceptable minima at three different wavelengths in the range $k_1 = (5.8 \pm 0.6) \times 10^{-4}$ s^{-1}, $k_2 = (2.0 \pm 0.5) \times 10^{-4}$ s^{-1} for reaction 12 and $k_1 = (9.0 \pm 0.9) \times 10^{-3}$ s^{-1}, $k_2 = (5 \pm 1) \times 10^{-3}$ s^{-1} for reaction 13.

The large spread in acceptable solutions is a result of correlation problems, which are common in this type of analysis.[27] To place

(27) Lingane, P. J.; Hugus, Z. Z. *Inorg. Chem.* **1970**, *9*, 757.

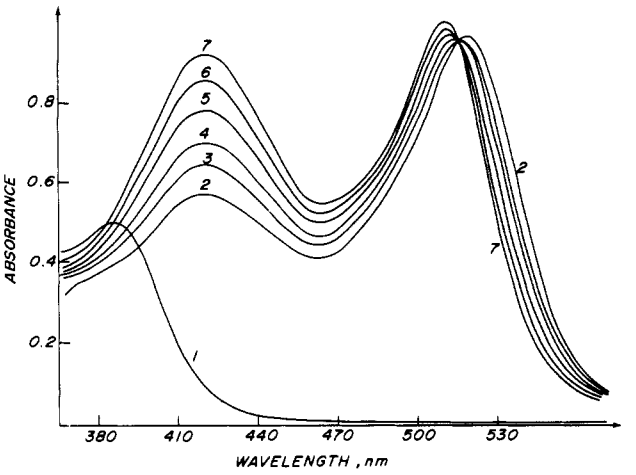

Figure 2. Spectral changes following the photolysis of $FeN_4(MeIm)(CO)$ (spectrum 1) in toluene solution containing 0.1 M py to generate $FeN_4(py)(MeIm)$ (spectrum 2) and its subsequent thermal reaction with excess py at 10 °C. Spectra 3–7 were recorded at times 15, 29.5, 63.5, 113, and 210 min after photolysis.

additional constraints on the solution the common intermediate $FeN_4(MeIm)(py)$ was generated photochemically from the carbonyl derivatives:

$$FeN_4(MeIm)(CO) \xrightarrow[+py]{h\nu} FeN_4(MeIm)(py) + CO \quad (14)$$

As shown in Figure 2 this approach gives a good spectrum of the intermediate $FeN_4(MeIm)(py)$, and the subsequent thermal reaction gives an independent measure of k_2 in reaction 12. The corresponding photochemical reaction of $FeN_4(py)(CO)$ with MeIm gives the same intermediate, and the subsequent thermal reaction with excess MeIm gives k_2 for reaction 13. Values of k_2 from this approach are within the range of acceptable solutions to the two-rate analysis above but are considered more accurate. The spectrum of the intermediate can be used to place additional constraints on A_2 in the above analysis. The values of k_1 for reactions 12 and 13 were also independently obtained by using $P(OBu)_3$ as the entering ligand, in which case only a single rate process is observed at 10 °C. In summary, the analysis of absorbance data for reaction 12 and 13 provide an acceptable range of solutions, which can be narrowed down considerably by using independent determinations of some of the parameters involved.

Substituted Pyridine Derivatives. Pyridine derivatives of FeN_4 show an additional band in the visible region, which is assigned to charge transfer to pyridine (MPyCT). This band is sensitive to substituents on the pyridine occurring at 530 nm for $FeN_4(4\text{-}CNPy)_2$ and at 370 nm for $FeN_4(4\text{-}Me_2NPy)_2$. In the mixed-ligand species $FeN_4(py)(L)$ two bands assigned to MPyCT to each of the pyridine ligands are typically observed. For example in $FeN_4(4\text{-}CNPy)(py)$, bands are found at ~535 nm (M → 4-CNPy) and 390 nm (M → py). The band at 390 nm assigned to change transfer to the py ligand is shifted somewhat from that in $FeN_4(py)_2$ and is less than one-half as intense. Kinetic data for reactions 15–19 for L = substituted pyridine are given in Table III.

$$FeN_4L_2 + P(OBu)_3 \rightarrow FeN_4(L)(P(OBu)_3) + L \quad (15)$$

$$FeN_4L(PR_3) + PR_3 \rightarrow FeN_4(PR_3)_2 + L \quad (16)$$

$$FeN_4L(py) + L \rightarrow FeN_4L_2 + py \quad (17)$$

$$FeN_4(4\text{-}NMe_2Py)(CO) + 4\text{-}NMe_2Py \rightarrow FeN_4(4\text{-}NMe_2Py)_2 + CO \quad (18)$$

$$FeN_4(4\text{-}CNPy)(CO) + 4\text{-}NMe_2Py \xrightarrow{slow} FeN_4(4\text{-}CNPy)(4\text{-}NMe_2Py) \xrightarrow{fast} FeN_4(4\text{-}NMe_2Py)_2 \quad (19)$$

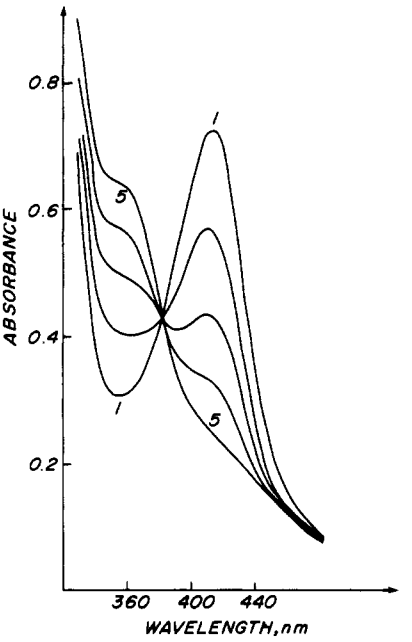

Figure 3. Spectral changes during the in situ generation of $FeN_4(P(OBu)_3)(CO)$ from $FeN_4(P(OBu)_3)_2$ at 60 °C in CO-saturated toluene. Spectra 1–5 were taken at 0, 3, 7, 12, and 23 min.

Addition of $P(OBu)_3$ to FeN_4L_2 proceeds in two distinct steps. Reaction 15 was followed at 10 °C. The subsequent slower reaction (eq 16) was studied at 45 °C.

The mixed ligand species $FeN_4L(py)$ was obtained by photolysis of $FeN_4(py)(CO)$ in the presence of excess L at 10 °C by the method described above for the $FeN_4(MeIm)(py)$ complex. Subsequent reaction to give FeN_4L_2 occurs with clean isosbestic points in a smooth first-order rate at 10 °C (reaction 17).

Although reaction 18 readily affords the desired CO off rate, the analogous reaction using $FeN_4(4\text{-}CNPy)(CO)$ and 4-CNPy results in a equilibrium due to the faster rate of the reverse reaction (see k_{-L} in Table III). This difficulty was avoided by carrying out reaction 19 where the first step, $k_{-CO}^{4\text{-}CNPy}$, is the rate-determining step and the reverse reaction is negligible.

Mixed-Ligand Species. The carbonyl complexes $FeN_4(PR_3)(CO)$ were obtained in situ by heating CO-saturated toluene solutions of the corresponding $FeN_4(PR_3)_2$ complexes (Figure 3):

$$FeN_4(PR_3)_2 + CO \rightleftarrows FeN_4(PR_3)(CO) + PR_3 \quad (20)$$
$$R = Bu \text{ or } OBu$$

Dilute solutions ([Fe] = 10^{-4} M) were required to drive the equilibria to the right at 1 atm of CO, and this fact also makes it difficult to obtain solid samples of the carbonyl complexes. Solutions of the carbonyls undergo clean reactions with excess PBu_3, $POBu_3$, BzNC, or MeIm, always giving initial replacement of CO at a rate constant $k_{-CO}^{PR_3}$. Reaction with MeIm results in replacement of CO initially but eventually gives an equilibrium mixture of $FeN_4(MeIm)(CO)$ and $FeN_4(MeIm)_2$ via three consecutive first-order reactions (Figure 4):

$$FeN_4(PR_3)(CO) + MeIm \xrightarrow{k_1} FeN_4(PR_3)(MeIm) \xrightarrow{k_2} FeN_4(MeIm)_2 \xrightarrow{k_3} FeN_4(MeIm)(CO) \quad (21)$$

Under the conditions of the experiment the values of three first-order rate constants are $k_1 = k_{-CO}^{PR_3}$, $k_2 = k_{-PR_3}^{N}$, and

$$k_3 = \frac{k_{-N}^{N}k_{+CO}^{N}[CO] + k_{-CO}^{N}k_{+N}^{N}[MeIm]}{k_{+N}^{N}[MeIm] + k_{+CO}^{N}[CO]} \quad (22)$$

Because of the slower rate for k_{-P}^{N} compared to k_{-PO}^{N} the buildup of the $FeN_4(MeIm)_2$ intermediate is less for PBu_3 compared to $P(OBu)_3$.

Mixed phosphine–phosphite complexes were also obtained in situ, making use of the trans effect order. Thus reaction 8 affords

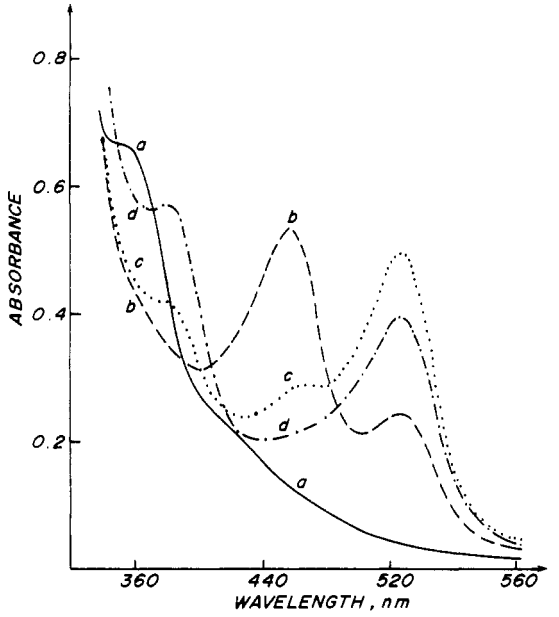

Figure 4. Spectral changes for reaction of $FeN_4(P(OBu)_3)(CO)$ at 45 °C in CO-saturated toluene solution containing 0.40 M MeIm. Spectra a–d were recorded at 0, 9, 55, and 115 min. Intervening spectra have been omitted for clarity. The three distinct steps in this reaction are described in the text (eq 21).

the desired mixed species since $k_{-P}^{PO} << k_{-P}^{P}$ while reaction 9 does not, going directly to the bis(phosphine) since $k_{-PO}^{P} >> k_{-PO}^{PO}$.

Similarly the reactions

$$FeN_4(PR_3)_2 + R'NC \rightarrow FeN_4(PR_3)(R'NC) \quad (23)$$

R = Bu or OBu R'NC = BzNC or TMIC

give the mixed phosphine–isocyanide species since the subsequent reaction to give $FeN_4(R'NC)_2$ is very slow.

Owing to the very slow rates for k_{-RNC}^{RNC}, mixed carbonyl–isocyanide complexes could not be obtained thermally. However a photochemical substitution reaction readily gives the desired complex:

$$FeN_4(BzNC)_2 \xrightarrow[CO]{h\nu} FeN_4(BzNC)(CO) + BzNC \quad (24)$$

Spectral data assigned to the photochemical reaction (eq 24) and the subsequent thermal reaction to give back the starting $FeN_4(BzNC)_2$ species are shown in Figure 5.

The assumption of a D mechanism was checked in a number of ways. We specify a few of them here. Several of the rates were studied as a function of the nature of the entering ligand. For example reactions of $FeN_4(P(OBu)_3)_2$ with excess CO, MeIm, py, PBu_3, and BzNC all proceed at the same rate. Where the off rates of the two axial ligands in a complex differ significantly, the product of the reaction with a third ligand corresponds to the reaction involving replacement of the more labile ligand. Thus

$$FeN_4(MeIm)(PBu_3) + BzNC \rightarrow FeN_4(PBu_3)(BzNC) + MeIm \quad (25)$$

while

$$FeN_4(MeIm)(P(OBu)_3) + BzNC \rightarrow FeN_4(MeIm)(BzNC) + P(OBu)_3 \quad (26)$$

as expected from k_{-P}^{N} vs. k_{-N}^{P} and k_{-PO}^{N} vs. k_{-N}^{PO} in Table II.

These characteristics were routinely made use of in our work.

It is virtually impossible for alternative dissociative pathways such as slow dissociation of the wrong ligand followed by fast dissociation of the correct one or a rate-determining step involving formation of a tetracoordinate species to complicate the kinetic determinations in this work.[14,16] The reaction of $Fe(DMGH)_2(PBu_3)(CO)$ with MeIm discussed above is an example of this "backdoor mechanism". However, since the rates are slow and each species is spectrally distinct, the presence of this mechanism is obvious. At 0.1 M ligand concentrations, the lifetime of the pentacoordinate species is probably $\sim 10^{-7}$ s. Thus complications associated with tetracoordinate species are unlikely. In most cases, the independence of the rate on the nature or concentration of the entering group also rules out complicating pathways.

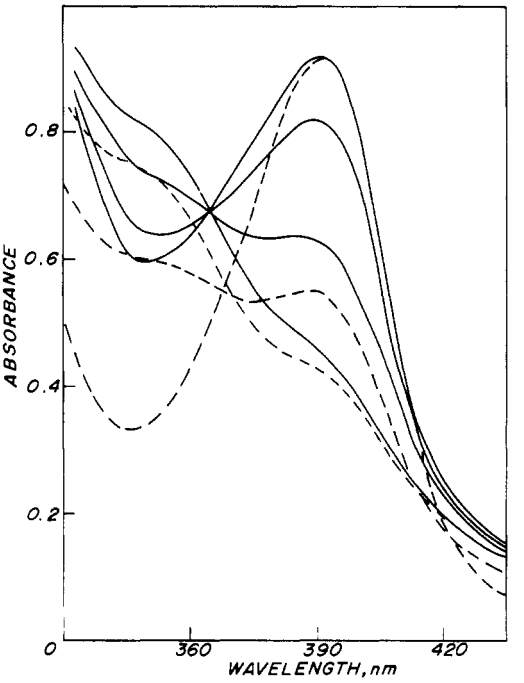

Figure 5. Spectral changes on successive photolysis of $FeN_4(BzNC)_2$ (λ_{max} = 392 nm) in CO-saturated toluene solution at 60 °C (--), eq 24, and the reverse reaction following addition of 0.1 M BzNC and nitrogen purge (—) at 0, 5, 14, and 25 min for increasing absorbance at 392 nm.

Table IV. Activation Parameters for Axial Ligand Substitution Reactions of FeN_4TL Complexes in Toluene[a,b]

T	L	$\Delta H^{\ddagger}$, kcal/mol	$\Delta S^{\ddagger}$, cal/(deg mol)	$\Delta G^{\ddagger}_{298}$, kcal/mol
MeIm	MeIm	25.7 (8)	17 (3)	20.5
MeIm	PBu_3[c]	33 (1)	25 (4)	25.6
MeIm	$P(OBu)_3$[d]	29.0 (2)	19 (1)	23.3
MeIm	CO[e]	26.8 (5)	7 (2)	24.7
py	CO[e]	28 (1)	14 (4)	23.8
$P(OBu)_3$	MeIm	30.9 (4)	19 (2)	25.2
PBu_3	MeIm	29.5 (1)	21 (2)	23.2
BzNC	py[e]	28.4 (7)	9 (2)	25.7
BzNC	MeIm[e]	31 (1)	12 (3)	27.4
TMIC	py[f]	31.2 (2)	16 (1)	26.4

[a] L is the leaving group and T is the trans ligand. [b] Numbers in brackets are the error in last digit of the data. [c] k_{obsd} at 45, 60, and 70 °C are 1.1×10^{-4}, 1.3×10^{-3}, and 4.9×10^{-3} s^{-1}, respectively. [d] k_{obsd} at 45, 60, and 70 °C are 8.4×10^{-4}, 6.8×10^{-3}, and 0.026 s^{-1} respectively. [e] Recalculated from data in ref 2 by using a linear least-squares fit. [f] k_{obsd} at 60, 80, and 90 °C are 5.8×10^{-5}, 1.1×10^{-3}, and 2.9×10^{-3}, respectively.

Activation Parameters. Rates studied as a function of temperature and the activation parameters obtained by a least-squares fit of ln (k/T) vs. $1/T$ are given in Table IV. Differences in rate are seen to be largely due to enthalpic factors and the $\Delta S^{\ddagger}$ are all positive and typically in the range +10 to +20 cal/(deg mol), typical of a dissociative mechanism where solvation effects are small.

On Rates. Kinetic data for several reactions studied under pseudo-first-order conditions in both entering and leaving ligands are summarized in Table V. In all cases the dependence of k_{obsd} on [E]/[L] is consistent with that expected from eq 4. Values of k_{+E}/k_{+L} obtained from eq 4 are summarized in Table VI. As an additional test of the D mechanism, a competitive trapping method was used. In the presence of two potential entering ligands

Table V. Dependence of k_{obsd} for the Reaction $FeN_4TL + E \rightarrow FeN_4TE + L$ on [E]/[L] in Toluene[a]

T	L	E	T, °C	[E]/[L]	$10^4 k_{obsd}$, s^{-1}
MeIm	MeIm	$P(Bu)_3$	25	1.3	15
MeIm	MeIm	$P(OBu)_3$	25	5.6	42
				2.3	23
				0.23	4.4
MeIm	MeIm	BzNC	25	0.52	28
MeIm	MeIm	TMIC	25	1.0	42
				0.53	33
				0.23	18
MeIm	MeIm	CO	25	1.8	11
				0.58	4.4
PBu_3	MeIm	$P(Bu)_3$	60	5.1	75
				2.5	52
				1.0	34
				0.8	29
PBu_3	PBu_3	BzNC	60	0.27	5.5
PBu_3	$P(OBu)_3$	PBu_3	60	0.88	24
$P(OBu)_3$	$P(OBu)_3$	PBu_3	60	0.88	6.9
$P(OBu)_3$	$P(OBu)_3$	CO	60	0.95	33
$P(OBu)_3$	CO	$P(OBu)_3$	60	0.58	91

[a] Error in k_{obsd} ±5%.

Table VI. Ratios of On Rates for Pentacoordinate Intermediates $FeN_4(X)$ (X = Tributyl Phosphite (PO), Tributylphosphine (P), and Methylimidazole (N)) in Toluene[a]

intermediate $Fe(DMGH)_2(X)$	T, °C	on rates
$Fe(DMGH)_2(MeIm)$	25	$k_{+N}/k_{+P} = 4$ (1)
		$k_{+N}/k_{+PO} = 4$ (1)
		$k_{+N}/k_{+BzNC} = 0.6$ (1)
		$k_{+N}/k_{+TMIC} = 0.5$ (1)
		$k_{+N}/k_{+CO} = 8$ (1)
		$k_{+P}/k_{+PO} = 0.7$ (3)[b,c]
		$k_{+P}/k_{+CO} = 1.7$ (7)[b,d]
		$k_{+PO}/k_{+CO} = 1.4$ (2)[b,e]
		$k_{+TMIC}/k_{+CO} = 15$ (3)[b,f]
$Fe(DMGH)_2(PBu_3)$	60	$k_{+N}/k_{+P} = 4$ (1)
		$k_{+P}/k_{+PO} = 1.2$ (3)
		$k_{+BzNC}/k_{+P} = 11$ (3)
$Fe(DMGH)_2(P(OBu)_3)$	60	$k_{+N}/k_{+PO} = 5$ (2)[g]
		$k_{+P}/k_{+PO} = 1.0$ (1)
		$k_{+PO}/k_{+CO} = 1.4$ (3)

[a] Calculated from eq 4 by using data in Tables II and V. [b] Obtained from product ratios determined from visible spectrum after the competition reaction of $\sim 10^{-4}$ M $FeN_4(MeIm)_2$ with two entering ligands under conditions described in footnotes *c–f*. [c] [P] = 0.0161 M; [PO] = 0.0118 M. [d] [P] = 4.03×10^{-3} M; [CO] = 7×10^{-3} M. [e] [PO] = 3.7×10^{-3} M; [CO] = 7×10^{-3} M. [f] [TMIC] = 6.8×10^{-4} M; [CO] = 7×10^{-3} M. [g] Calculated from data in Table II and eq 5 by using $K = 0.09 \pm 0.03$ obtained spectrophotometrically.

E_1 and E_2, the pentacoordinate intermediate will form products in the ratio of the rates of addition of the ligands:

$$\frac{[FeN_4T(E_1)]}{[FeN_4T(E_2)]} = \frac{k_{+E1}^{T}[E_1]}{k_{+E2}^{T}[E_2]} \qquad (27)$$

The relative concentrations of the two products may be obtained from an analysis of the visible spectrum of the resulting mixture in favorable cases.

One example of this method is shown in Figure 6.

$$FeN_4(MeIm)_2 \underset{k_{+N}^{N}}{\overset{k_{-N}^{N}}{\rightleftharpoons}} FeN_4(MeIm) \xrightarrow[+P(OBu)_3]{k_{+PO}^{N}} FeN_4(MeIm)(P(OBu)_3) \qquad (28)$$

$$FeN_4(MeIm) \xrightarrow[+CO]{k_{+CO}^{N}} FeN_4(MeIm)(CO)$$

The extent to which the intermediate is trapped as $FeN_4(MeIm)(P(OBu)_3)$ or $FeN_4(MeIm)(CO)$ is deduced from the absorbances at 460 and 385 nm, respectively. The presence of clean isosbestic points is expected in a case where two products

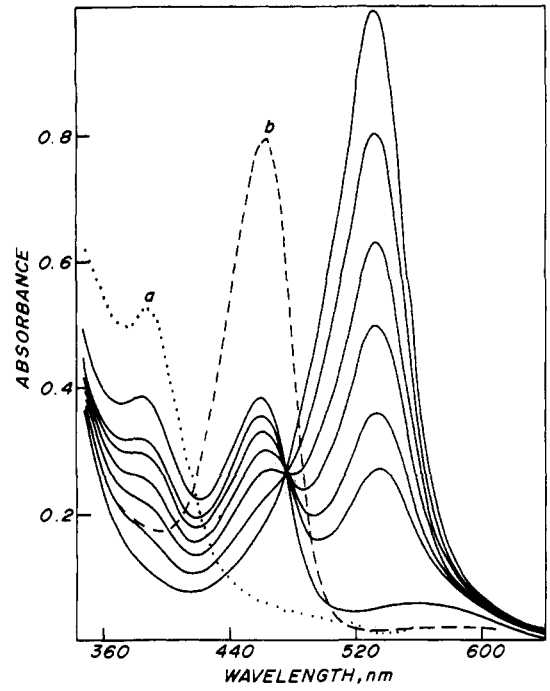

Figure 6. Spectral changes during the reaction of $FeN_4(MeIm)_2$ in toluene containing CO (7×10^{-3} M) and $P(OBu)_3$ (3.7×10^{-3} M). Relative amounts of $FeN_4(MeIm)(CO)$ (λ_{max} = 385 nm) and $FeN_4(MeIm)(P(OBu)_3)$ (λ_{max} = 460 nm) were deduced from spectra for the corresponding reaction with only CO (···) or only $P(OBu)_3$ (- -).

are formed in a constant ratio with time.[28] Potentially complicating secondary reactions including k_{-N}^{PO}, k_{-PO}^{N}, k_{-CO}^{N}, and k_{-N}^{CO} are all negligibly slow at 10 °C (Table II). In some cases an excess of MeIm was used, in which case the third path (k_{+N}^{N}) is important in reaction 28. Equation 27 is still valid under these conditions.

A similar photochemical trapping method wherein the intermediate is generated by photolysis of $FeN_4(MeIm)(CO)$ gives identical results. These will be described elsewhere[22] in conjunction with quantum yield studies.

Discussion

The position of the visible spectral maximum assigned to Fe to oxime charge transfer is a sensitive measure of the donor–acceptor properties of the axial ligands. The band position is to a small extent a function of global d orbital shifts arising from net electron density on the iron[29] but primarily results from the lowering of $d_{xz,yz}$ due to π bonding to the axial ligands. Assuming the π-bonding effect dominates, this gives a π-acceptor order CO > TMIC > BzNC > $P(OBu)_3$ > PBu_3 > MeIm, py.

Kinetics. An abundance of evidence for the assumed dissociative mechanism has been presented in the Results section and will not be further elaborated upon.

Off rates depend upon the leaving group and the trans ligand. The leaving group order is py > MeIm > $P(OBu)_3$ > PBu_3 > BzNC,TMIC ≈ CO. With the exception of the position of CO, this order is essentially the same as found in several other iron(II) systems including hemes,[6,30–32] phthalocyanines,[7–9] TIM,[10–14] and other dioximes.[4,21]. Furthermore a similar order, py > $P(OMe)_3$) > CO > PBu_3, is found in $Cr(CO)_5L$ complexes.[33]

Trans Effects. The trans effects shown in Table II reinforce and extend previous results, which show π acceptors are strongly trans delabilizing in FeN_4 systems.[4,6–10,12–14] In making comparisons within Table II, values reported at 80 °C should be divided by ~10 for direct comparison with the other constants

(28) Stynes, D. V. *Inorg. Chem.* **1975**, *14*, 453.
(29) For example, see shifts for substituted pyridine derivatives in Table III.
(30) Fletcher, D.; Stynes, D. V., unpublished results on PR_3 binding.
(31) Brault, D.; Rougee, M. *Biochem. Biophys. Res. Commun.* **1974**, *57*, 654.
(32) Stynes, D. V. *J. Am. Chem. Soc.* **1974**, *96*, 5942.
(33) Wovkulich, M. J.; Atwood, J. D. *J. Organomet. Chem.* **1980**, *77*, 1184.

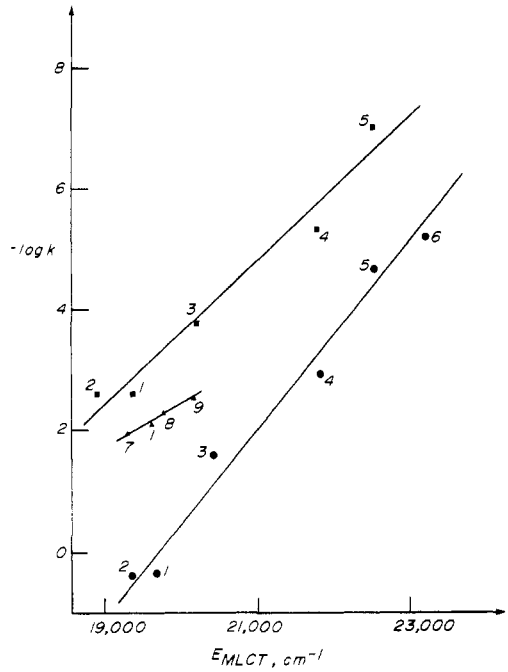

Figure 7. Correlation of off rates of methylimidazole and pyridine trans to T (T = py (1), MeIm (2), PBu_3 (3), $P(OBu)_3$ (4), BzNC (5), TMIC (6), 4-CNPy (7), 3,4-Me_2Py (8), and 4-NMe_2Py (9)) with E_{MLCT}: (■) $k_{-N}^{T} \times 10^{-2}$, 60 °C; (▲) k_{-Py}^{T}, 10 °C; (●) k_{-Py}^{T}, 45 °C.

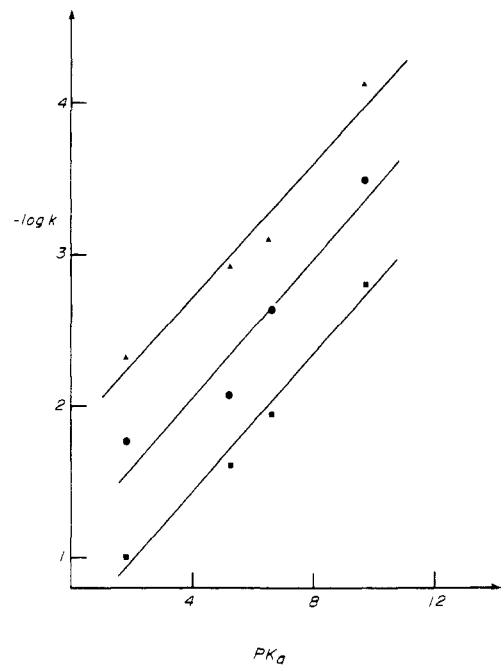

Figure 8. Correlation of off rates of substituted pyridines trans to py (●, 10 °C), PBu_3 (■, 45 °C), or $P(OBu)_3$ (▲, 45 °C) with pK_a.

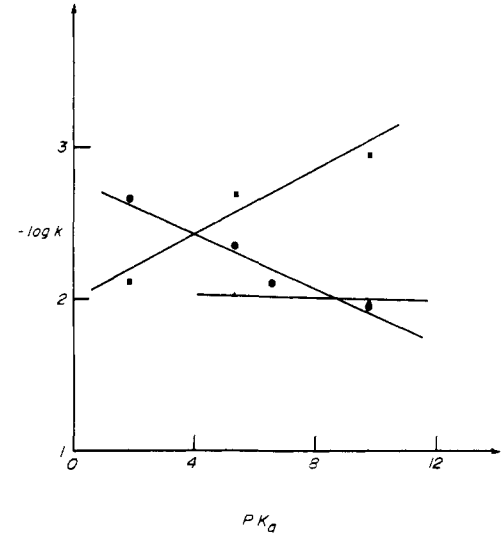

Figure 9. Correlation of the trans effect of substituted pyridines with pK_a on the off rates of py (●, 10 °C), $P(OBu)_3$ (▲, 60 °C), or CO (■, 60 °C).

at 60 °C. Also diagonal entries should be divided by 2 in order to correct for statistical effects.

For the strictly σ-donor ligands MeIm and py there is almost no trans effect of these ligands on each other after correction for the statistical factor of 2. Trans effects of the π-acceptor ligands on k_{-py} and k_{-N} are much larger, with lability decreasing from left to right in the table. A linear correlation between the energy of the MLCT band and log k_{-py}^{T} and log k_{-N}^{T} is observed (Figure 6). Assuming the correlation extends to the trans ligand CO, values of k_{-Py}^{CO} at 45 °C and k_{-N}^{CO} at 60 °C are calculated to be 5×10^{-8} s^{-1} and 5×10^{-10} s^{-1}. These extrapolated values are consistent with our inability to observe any ligand dissociation trans to CO in this work. In all cases an upper limit on k_{-X}^{CO} would be the value of k_{-CO}^{X}. The relative trans effects of PBu_3 and $P(OBu)_3$ are consistent with the greater π-acceptor ability of $P(OBu)_3$. It is seen that the trans effect is not simply related to the metal–ligand bond strength of the trans ligand since PBu_3 binds more strongly than $P(OBu)_3$ but is more trans labilizing while BzNC binds more strongly than $P(OBu)_3$ and is less trans labilizing. The correlation of the trans effect order with the π-acceptor character of the ligand as measured by E_{MLCT} (Figure 7) is evidence that a significant weakening of the π bonding to the trans ligand occurs on loss of the trans σ donors MeIm and py. This effect decreases substantially in magnitude for the leaving groups PBu_3, $P(OBu)_3$, and RNC and shows a reversal and a more complex dependence for k_{-CO}^{T}.

Probably closely related to the trend in trans effects in FeN_4 systems are observations on the relative binding affinity of ligands to hemes trans to a nitrogen donor vs. those trans to a void. Binding to the open face of capped hemes provides a simple way of obtaining equilibrium constants trans to a void although some caution should be exercised in making comparisons to flat hemes.[16] Values of log K_B for py, MeIm, PBu_3, $P(OBu)_3$, and BzNC are 1.88, 2.90, 4.66, 3.24, and 5.44 for Fe(cap)[34] and 4.82 for CO in FeTPP.[31] Typical values for ligands trans to N for log K^{N}_{B} are 4.9 (Im),[35] 8.6 (BuNC or CO),[16] and 5.74 ($P(OBu)_3$).[30] These data show that π acceptors bind more poorly trans to a void than trans to a good σ donor in approximate proportion to their π-acceptor ability. This fact is clearly significant in the barrier for a ligand dissociation that creates a void trans to the ligand T. Both sets of data point to the importance of a synergistic interaction between a good σ donor and a good π acceptor in mutually trans positions. Because of this, the barrier to MeIm or py dissociation depends as much on the resultant weakening of the Fe–T bond in going to the transition state, as on the inherent Fe–N ground-state bond strength. This effect is dramatically different when T is a σ donor since generally a metal–ligand σ bond increases slightly in strength as the coordination number decreases.

Substituted Pyridines. Data for the substituted pyridine derivatives presumably reflect primarily σ effects. The leaving group order trans to $P(OBu)_3$ and PBu_3 correlates with the basicity of the pyridine (Figure 8). A similar trend is found for k_{-L}^{L} if a correction for the different trans effects of L is made.

The trans effects plotted in Figure 9 depend on the nature of the leaving group. The strong σ donor 4-Me_2NPy is trans labilizing compared to 4-CNPy for loss of py. This smaller effect is usually interpreted in terms of a ground-state effect[36,37] wherein

(34) Ellis, P. E., Linard, J. E.; Symanski, T.; Jones, R. D.; Budge, J. R.; Basolo, F. *J. Am. Chem. Soc.* **1980**, *102*, 1889.
(35) Brault, D.; Rougee, M. *Biochemistry* **1975**, *14*, 4100.
(36) Burdette, J. K.; Albright, T. A. *Inorg. Chem.* **1979**, *18*, 2117.

Table VII. Comparison of On Rates for Hemes with Those Calculated for $Fe(DMGH)_2$ Complexes[a]

X	$10^{-7}k_{+X}$, M^{-1} s^{-1}	
	heme	DMGH
MeIm	18[b]	18[a]
BzNC	22[c,d]	30
TMIC	17[c]	36
CO	1.1[c]	2.2
PBu_3		4.5
$P(OBu)_3$		4.5

[a] A value for $k_{+N}^{N} = 1.8 \times 10^8$ M^{-1} s^{-1} is assumed for $Fe(DMGH)_2$ at 25 °C. Values are calculated from relative on rates in Table VI. No corrections are made for temperature differences. [b] FeTPP; ref 15. [c] Chelated protoheme; ref 6 and 16. [d] The value given is for BuNC, which is expected to be similar to that for BzNC.[20]

the stronger σ donor acquires a greater share of the metal acceptor orbitals at the expense of the weaker ligand in the trans position. Corresponding trans effects on $P(OBu)_3$ dissociation are very small, and for the strong π acceptor, CO, the trans effect order is reversed. The stronger base 4-Me_2NPy enhances CO binding compared to 4-CNPy. These trends are reflected in the slopes of the lines in Figure 9.

On Rates. Relative rates of addition of ligands to the pentacoordinate intermediates have generally been found to be close to unity,[7,9,10] indicative of a rapidly reacting nondiscriminating species, as might be expected for addition to a vacant coordination site.[38] On rates have been best characterized in hemes where direct determinations using flash photolysis methods can be easily applied.[15-20] While large differences in on rates as a result of steric effects have been definitely established,[26] smaller differences in rates for unhindered systems as a function of the ligand being added have not been extensively discussed. Lavalette[15] has attempted to rationalize an inverse dependence of on rates for substituted pyridines with basicity in terms of dipolar effects. However other factors must be involved since the ligand that adds most slowly to hemes is CO and it has a negligibly small dipole moment. In fact Olsen[20] has used the same dipolar argument in exactly the opposite sense to explain why isocyanides add faster than CO to hemes!

Table VII compares known on rates of ligands to hemes with comparable data in the dimethylglyoxime complexes. On rates from this work are obtained by arbitrarily assuming $k_{+N} = 1.8 \times 10^8$ M^{-1} s^{-1} (the same as hemes) and calculating the remaining on rates from the ratios in Table VI. The table shows a striking similarity in the two systems with CO adding about 10 times slower than methylimidazole in both. On the other hand, the other carbon donor ligands, isocyanides, add at least as fast as methylimidazole in both systems.

In our work the relative on rates are not sensitive to the nature of the trans ligand. We are reluctant to include data in other solvents since we expect solvent effects may be significant, but the data of Sweigart[9] for iron phthalocyanine in acetone also indicate slight discrimination factors involving MeIm, py, PBu_3, and $P(OBu)_3$ as ligands (less than a 2-fold variation) and no detectable dependence on the trans ligand.

There is an insufficient data base to offer definitive explanations for the small differences in on rates observed in these systems. However, some more dramatic differences in heme systems point to some of the important factors. Addition to flat tetracoordinate hemes is much faster than to pentacoordinate high-spin hemes.[6] $k_{+CO} = 5.7 \times 10^8$ M^{-1} s^{-1} and $k_{+Im} = 9 \times 10^8$ M^{-1} s^{-1} compared to $k_{+CO}^{IM} = 1.2 \times 10^7$ M^{-1} s^{-1}. Addition of Im to low-spin Fe(DHD)(CO)[6] is about the same as addition to high-spin FeTPP(Im).[15] These results coincide with conclusions from the $Fe(DMGH)_2$ system that on rates are relatively insensitive to the trans ligand unless the trans ligand is a void.

General Application to Organometallics. The trans effect information in Table II may be used to test some of the qualitative notions widely used in the organometallic chemistry of metal complexes of the ligands considered in this work.

The principle of antisymbiosis[41] states that "two soft ligands in mutually trans positions on a soft metal center will destabilize each other". Consider the equilibrium

$$FeN_4(PBu_3)_2 + FeN_4(MeIm)_2 \rightleftarrows 2FeN_4(PBu_3)(MeIm) \quad (29)$$

The overall equilibrium constant is given by

$$K = \frac{k_{-N}^{N} k_{-P}^{P} k_{+N}^{P} k_{+P}^{N}}{k_{-N}^{P} k_{-P}^{N} k_{+N}^{N} k_{+P}^{P}} \quad (30)$$

The on rate ratios are relatively independent of the trans ligand (Table VII), and thus the position of this equilibrium is governed by the off rates. Using data at 60 °C from Table II, we obtain $K = (5200)(7.5)/(158)(13) = 19.0$. This equilibrium lies to the right but violates the principle of antisymbiosis. The Fe–P bond is actually more inert in the $FeN_4(PBu_3)_2$ species than in the $FeN_4(MeIm)(PBu_3)$ complex.

Another commonly invoked idea primarily originating from data on CO stretching frequencies is that two π acceptors in mutually trans positions exert a destabilizing effect. Consider the equilibrium

$$FeN_4(PBu_3)_2 + FeN_4(P(OBu)_3)_2 \rightleftarrows 2FeN_4(PBu_3)(P(OBu)_3) \quad (31)$$

where

$$K = \frac{k_{-P}^{P} k_{-PO}^{PO} k_{+PO}^{P} k_{+P}^{PO}}{k_{-P}^{PO} k_{-PO}^{P} k_{+P}^{P} k_{+PO}^{PO}} \quad (32)$$

Assuming the ratio of on rates is unity, we obtain $K = 14$ for equilibrium 31. This is the expected direction on the basis of the proposed destabilizing effect of the good π acceptor $P(OBu)_3$ in $FeN_4(P(OBu)_3)_2$, but the individual rate constants indicate the proposed reason is wrong. In fact, the major factor in the above is the 37.5-fold smaller value of k_{-P} for ligands trans to $P(OBu)_3$. The proposed π destabilization is not present since $k_{-PO}^{PO} < k_{-PO}^{P}$.

Only in the rate of loss of CO do we see a deviation from the general trans effect order, and even here a strictly π-bonding effect does not adequately account for the rates. For example the weaker π acceptor PBu_3 gives a more labile CO than does $P(OBu)_3$, and benzylisocyanide has an effect similar to pyridine. Unfortunately the σ-donor properties of CO and RNC are less well understood than their π-bonding characteristics, making a more definitive discussion difficult.

The arguments above based on a detailed analysis of mutual trans effects apply *only* to dynamic aspects of metal complexes. In the sense that thermodynamic stability depends on forward and reverse rate constants, this includes equilibrium constants, $\Delta G°$, and $\Delta H°$. The rate constants do not necessarily indicate anything about bond lengths, vibrational data, coupling constants, or other spectroscopically derived data often cited as evidence of static trans effects.

A general rule that emerges from this work is that the barrier for dissociation of a ligand from an 18-electron low-spin d^6 complex is critically dependent upon the net electron donor properties of the other ligands bound to the metal and the trans effects are largest on the strongest net donor in the complex. A similar conclusion based on a more limited data set for chromium carbonyl complexes is presented by Atwood.[42] Where data is available

(37) Shustorovich, E. M.; Porai-Koshits, M. A.; Buslaev, Y. A. *Coord. Chem. Rev.* **1975**, *17*, 1.
(38) For example rate constants are reported for the following: addition of CO to tricoordinate $Rh(PPh_3)_2Cl$ in benzene,[39] $k_{+CO} = 6 \times 10^7$ M^{-1} s^{-1}; addition of CO and H_2O to $Cr(CO)_5$ in cyclohexane,[40] $k_{+CO} = 3.6 \times 10^6$ M^{-1} s^{-1} and $k_{+H_2O} = 4.6 \times 10^7$ M^{-1} s^{-1}. The corresponding gas-phase rate for CO addition to "naked" $Cr(CO)_5$ is 1.5×10^{10} M^{-1} s^{-1}.[41]
(39) Wink, D.; Ford, P. C. *J. Am. Chem. Soc.* **1985**, *107*, 1794.
(40) Church, S. P.; Grevels, F. W.; Hermann, H.; Schaffner, K. *Inorg. Chem.* **1985**, *24*, 418.
(41) Seder, T. A.; Church, S. P.; Ovderkirk, A. J.; Weitz, E. *J. Am. Chem. Soc.* **1985**, *107*, 1432.
(42) Pearson, R. G. *Inorg. Chem.* **1973**, *12*, 712.
(43) Atwood, J. D.; Wovkulich, J. J.; Sonnenberger, D. C. *Acc. Chem. Res.* **1983**, *16*, 350.

and where it is uncomplicated by cis labilization, the trans effects and leaving group trends in d^6 carbonyl complexes of Cr, Mo, and W are remarkably similar to our results on FeN_4 systems. This suggests that unifying principles covering organometallic as well as classical complexes might be found if sought. At the present time, there is very little overlap in the types of ligands and solvents used in these two major areas of inorganic chemistry. Complexes of the type considered here may provide a bridge between the chemistry of classical Werner complexes and organometallic compounds.

(44) Schofield, K. "Hetero-Aromatic Nitrogen Compounds"; Plenum Press: New York, 1967; p 146.

Acknowledgment. Support of the Natural Sciences and Engineering Research Council of Canada is gratefully acknowledged.

Registry No. $FeN_4(py)_2$, 24828-75-9; $FeN_4(MeIm)_2$, 57804-36-1; $FeN_4(MeIm)CO$, 61395-33-3; $FeN_4(BzNC)_2$, 59575-75-6; $FeN_4(MeIm)(py)$, 100466-68-0; $FeN_4(PBu_3)(py)$, 100485-19-6; $FeN_4(P(OBu)_3)(py)$, 100485-20-9; $FeN_4(BzNC)(py)$, 61395-34-4; $FeN_4(TMIC)(py)$, 100485-21-0; $FeN_4(py)CO$, 54691-99-5; $FeN_4(PBu_3)(MeIm)$, 100485-22-1; $FeN_4(P(OBu)_3)(MeIm)$, 100485-23-2; $FeN_4(BzNC)(MeIm)$, 59575-74-5; $FeN_4(TMIC)(MeIm)$, 100485-24-3; $FeN_4(PBu_3)_2$, 100485-25-4; $FeN_4(P(OBu)_3)(PBu_3)$, 100485-26-5; $FeN_4(BzNC)(PBu_3)$, 100485-27-6; $FeN_4(TMIC)(PBu_3)$, 100485-28-7; $FeN_4(PBu_3)CO$, 100485-29-8; $FeN_4(P(OBu)_3)_2$, 100485-30-1; $FeN_4(BzNC)(P(OBu)_3)$, 100485-31-2; $FeN_4(TMIC)(P(OBu)_3)$, 100485-32-3; $FeN_4(P(OBu)_3)CO$, 100485-33-4; $FeN_4(BzNC)CO$, 100485-34-5.

Contribution from the Department of Chemistry, Texas A&M University, College Station, Texas 77843

Reactions of Dioxygen Complexes. Oxidative Dehydrogenation of 2-(Aminomethyl)pyridine through Cobalt Dioxygen Complex Formation

Arup K. Basak and Arthur E. Martell*

Received October 14, 1985

The metal complex formation constants and the oxygenation constants of the cobalt(II) complexes of diethylenetriamine (DIEN) and 2-(aminomethyl)pyridine (AMP) have been determined by potentiometric measurements under N_2 and O_2. In the mixed-ligand systems three cobalt complexes are formed that are capable of combining with dioxygen: the 2:1 AMP complex, the 1:1:1 DIEN–AMP complex, and the 1:1 DIEN complex. The equilibrium constants for the mixed-ligand system have been employed to determine the conditions under which the concentration of the mixed-ligand complex has its maximum value and the conditions that favor the formation of the corresponding μ-peroxo cobalt complex. The kinetics of oxidative dehydrogenation of coordinated AMP through the formation and degradation of the mixed-ligand peroxo complex have been measured spectrophotometrically, and rate constants are reported. The reaction has been found to be second order, first order in the dioxygen complex and first order in the concentration of hydroxide ion. The reaction product in the two-electron oxidation of AMP is the corresponding imine, which under the reaction conditions employed is converted to pyridine-2-carboxaldehyde, determined quantitatively as the (2,4-dinitrophenyl)hydrazone. The proposed reaction mechanism involves deprotonation of the amino group, through the influence of the Co^{3+} center, as a preequilibrium step. This is followed by a concerted process involving homolytic fission of dioxygen, shift of an electron through the metal ion to the coordinated oxygen, and transfer of the α-proton to the coordinated oxygen atom. The two-electron oxidation of each AMP ligand is thus balanced by conversion of half of the dioxygen to water, with regeneration of cobalt(II). The proximity of the dioxygen to the α-CH_2 of the ligand is considered an important requirement for this concerted mechanism. The determination of large kinetic deuterium isotope effects (ca. 13–16) for the dehydrogenation rate constants seems to support the proposed mechanism.

Introduction

Polyamine complexes of cobalt(II) form binuclear dioxygen adducts having wide variations in thermodynamic stabilities and cobalt–dioxygen bond strengths.[1-4] With a large number of such complexes now available, it is of interest to examine their effectiveness as oxidants for hydroxylation and oxidative dehydrogenation of organic compounds. An important limiting factor in such studies is the tendency for all oxygen complexes to be converted to stable, inert complexes in which the coordinated ligand is oxidized, or the metal ion is oxidized to its higher valent form, and thus is no longer able to combine with dioxygen. Recently, bipyridyl was employed as a relatively refractory ligand for cobalt(II), resulting in the formation of a dioxygen complex, tetrakis(bipyridyl)(μ-peroxo)(μ-hydroxo)dicobalt(III), which is converted to inert dipyridylcobalt(III) complexes very slowly and is not appreciably decomposed during kinetic studies of its reactivity in the oxidation and oxygenation of 2,6-di-*tert*-butylphenol.[5] In a more recent kinetic study of the oxygenation and oxidative dehydrogenation of 2,6-di-*tert*-butylphenol by dioxygen complexes of a series of (polyamine)cobalt(II) complexes, it was found that quantitative determination of rate constants was not feasible for a number of relatively weak dioxygen complexes that undergo considerable decomposition during the course of the measurements.[6]

Because the rates of autoxidation reactions of μ-peroxo-bridged cobalt complexes are the limiting factors in catalytic oxidation and oxygenation studies, attention has recently been focused on the rates, reaction pathways, and mechanisms of these reactions.[7-10] With the coordinated polyamine ligands 1,9-bis(2-pyridyl)-2,5,8-triazanonane (PYDIEN) and 1,11-bis(2-pyridyl)-2,6,10-triazaundecane (PYDPT), oxidative dehydrogenation of the coordinated polyamine was found to occur during the autoxidation process.[7,10] With the pentadentate polyamines 2,6-bis(2-(3,6-diazahexyl))pyridine (EPYDEN), 1,9-bis(4-imidazolyl)-2,5,8-triazanonane (IMDIEN), and tetraethylenepentamine (TETREN), the autoxidation pathway was found to be entirely different in that, under the same reaction conditions, these coordinated ligands are not oxidized by coordinated dioxygen.[8-10] In the case of EPYDEN, which is a pyridyl-containing pentaamine, as are PYDIEN and PYDPT, the difference in reactivity seemed to be due to the conformation of the ligand in the dioxygen complex, which was not suitable for double-bond formation

(1) McLendon, G.; Martell, A. E. *J. Chem. Soc., Chem. Commun.* **1975**, 223.
(2) Harris, W. R.; Timmons, J. H.; Martell, A. E. *J. Coord. Chem.* **1979**, *8*, 251.
(3) Martell, A. E. *Acc. Chem. Res.* **1982**, *15*, 155.
(4) Niederhoffer, E. C.; Timmons, J. H.; Martell, A. E. *Chem. Rev.* **1984**, *84*, 137.
(5) Bedell, S. A.; Martell, A. E. *Inorg. Chem.* **1983**, *22*, 364.
(6) Bedell, S. A.; Martell, A. E. *J. Am. Chem. Soc.* **1985**, *107*, 7909.
(7) Raleigh, C. J.; Martell, A. E. *Inorg. Chem.* **1985**, *24*, 142.
(8) Raleigh, C. J.; Martell, A. E. *J. Chem. Soc., Chem. Commun.* **1984**, 335.
(9) Raleigh, C. J.; Martell, A. E. *J. Coord. Chem.* **1985**, *14*, 139.
(10) Raleigh, C. J.; Martell, A. E. *Inorg. Chem.*, in press.

0020-1669/86/1325-1182$01.50/0